# Site selective surface enhanced Raman on nanostructured cavities

Frances Lordan, James H Rice
*School of Physics, University College Dublin, Belfield, Dublin 4, Ireland*

Bincy Jose, Robert J Forster, Tia E Keyes
*School of Chemical Sciences, Dublin City University, Dublin 9, Ireland*

**abstract**

Presented here are angle dependence studies on the surface enhanced Raman (SER) signal obtained from dye placed on plasmon active nanocavity arrays. A comparative study was carried out between two modified array supports. One array had dye placed only on the interior walls of the cavities in the array. The other array had dye placed only on its top flat surface. Results show that Raman intensities as a function of angle depend on the location of the dye on the array; this was interpreted to arise from the presence of different plasmon polariton modes in these sites

**paper**

There is presently great interest in using uniform nanostructured surfaces to give reproducible plasmonic enhancement of the Raman signal of a sample.[1,2] The Raman signal is an extremely useful analytical tool as it provides a unique spectrum for molecules.[3] However, Raman scattering is a weak process and significant enhancement is required to make it more broadly applicable in analytical science. The nanostructured surfaces studied here have spherical cap architecture and are arranged uniformly in a gold array. Au is commonly used for plasmonic platforms as it produces chemically and structurally stable high quality arrays with visible plasmonic absorbance.[4] Furthermore, Au nanocavity arrays tend to be more reproducible and homogeneous than arrays made from other materials e.g. Ag.[5] Localised surface plasmon polaritons (LSPPs) exist inside the nanocavities and both localised and delocalised (propagating) surface plasmon polaritons (PSPPs) exist on the flat surface of the sample. The relative contribution from each plasmon type appears to depend on the dimensions of the cavity.[6] Studies on localised and delocalised plasmons have been carried out by Kelf et al. In these studies the contributions of the different plasmon types were investigated by varying the normalised sample film thickness. Other interesting studies on nanocavity arrays have been carried out by Chan et al in which the effect of cavity diameter (with fixed thickness Ag film) on the SERS intensity from a Ag array was investigated.[7]

Studies have been carried out on both the angle dependence of SERS and surface enhanced luminescence (SEL) from plasmon active nanocavity arrays.[8-15] These studies show that both SERS and SEL are dependent on the angle of laser incidence and/or detection angle. Such studies have been useful to elucidate the types of surface plasmon modes present on these cavities. Nanovoid substrates were reported to support localised (Mie) or delocalised (Bragg)

plasmons depending on the dimensions of the nanovoids themselves.[15] Bragg plasmons were shown to be present for thin films while localised Mie plasmons were seen at larger thicknesses. The presence of such modes has been observed in the near-field using scanning tunnelling microscopy (STM).[4] This approach distinguished between propagating SPP modes on the surface of the nanovoid substrate and localised Mie-type modes inside the voids. To date, while studies have been performed investigating the SER properties of these substrates, no studies on the angle dependence of the SER spectrum from the selectively modified arrays described here have been carried out.

Recently a protocol was reported in which a dye was attached at the top surface and separately at the internal cavity walls of a gold nanocavity array using a polystyrene sphere template. This protocol was used here to selectively modify the arrays. The externally modified array had Raman active dye placed only on the flat top surface of the array. The internally modified array had the dye placed only on the internal walls of the cavities. This enabled comparison between Raman spectra from dye localised in the cavity and spectra from dye attached to the top surface of the array. It also enabled comparison of the angle dependence of both spectra. This was done for arrays of cavity diameter 820nm. This study has the potential to enable clearer understanding of the distribution of the void and surface bound plasmon modes and to provide an insight into the angle dependence of excitation of modes located specifically at the top and cavity regions of the array. Results confirm that Raman signals depend on where the dye is located on the nanocavity array.

Gold nanocavity arrays on silicon wafer were prepared using a nanosphere lithographic technique based on electrodeposition through the voids of self-assembled polystyrene spheres as described previously.[1] Selective modification of the external edges and interior walls of the cavity arrays with $[Ru(bpy)_2(Qbpy)]^{2+}$ was achieved through a two step adsorption process. A spontaneously adsorbed monolayer of $[Ru(bpy)_2(Qbpy)]^{2+}$ was assembled on the top surface by placing the nanocavity array, with the templating polystyrene beads still in place, in a 1mM methanolic solution of the adsorbate overnight. The monolayer coated substrate was then sonicated in tetrahydrofuran (THF) for 1 hour to dissolve the templating spheres. $[Ru(bpy)_2(Qbpy)]^{2+}$ was adsorbed only at the internal cavity walls by exposure of the arrays to a solution of $[Ru(bpy)_2(Qbpy)]^{2+}$ after first modifying the edges with 1-nonanethiol. The templating spheres were then removed and the interior of the cavity was filled with a solution containing $[Ru(bpy)_2(Qbpy)]^{2+}$. The array was then allowed to stand in contact with this solution overnight to allow the spontaneously adsorbed molecule to form. Any excess physisorbed molecules were removed from the substance by sonication in a blank solvent and rinsing prior to measurements. $[Ru(bpy)_2(Qbpy)]^{2+}$ was synthesized from cis-$[Ru(bpy)_2Cl_2]$ as described previously.[16] This selective modification process is described in detail by Jose et al.[17] We demonstrate here how this selective modification enables comparison of the variation in SERS intensity of $[Ru(bpy)_2(Qbpy)]^{2+}$ over a range of angles for externally modified and internally modified arrays.

The sample was mounted onto a customised goniometer at a tilted angle of 13.5 degrees. The sample was excited at 633 nm with the laser focused using a 10 cm focal length lens. The Raman signals were collected at a backscattered angle and directed onto an electron multiplying charge coupled device (EMCCD) via a monochromator. Spectra were accumulated for 30 seconds. The

pump angle was varied in steps of 2 degrees and a spectrum was taken at each step. This was done for the 820nm diameter externally modified and internally modified cavity arrays.

An AFM topography image recorded of the sample is shown in Fig 1(a). The AFM used was a commercial AFM instrument series VICO explora and images were recorded in contact mode. The image shows the presence of the cavities on the sample surface. The cavities are 820 nm diameter spherical cap in structure. These cavities are present across the sample surface with approximately 10% of the surface defective in a 1 $mm^2$ area. The surface features possess an aspect ratio (of depth of coverage to diameter) of $\bar{t}$ =0.12.[6] The array dimensions were investigated as reported previously.[1]

SERs spectra recorded using a 633 nm excitation wavelength are shown in Figs 1(b) and 1(c). The Raman spectra show several peaks which are characteristic of pyridine modes observed previously from SERs spectra of $[Ru(bpy)_2(Qbpy)]^{2+}$.[1] The optical absorption spectrum of $[Ru(bpy)_2(Qbpy)]^{2+}$ is shown in Fig 1(d). The spectrum shows that small absorption intensity is present at 633 nm. Fig 1 shows SERs from $[Ru(bpy)_2(Qbpy)]^{2+}$ prepared (b) in the voids of the array and (c) on the surface of the array.

Fig 1(a) shows schematically the location of different plasmon modes that occur on the nanovoid array substrates. The red lines shown on Fig 1(a) indicate the possible paths of SPs on the array (marked 1 and 2 in Fig 1(a)) along with void localised plasmons (marked 3 in Fig 1(a)). Line 1 shows the path taken by a localised SP; it is localised by the nanocavity edges and is confined to the distance between the cavities. This localisation of the SP enables its contribution to the SER spectrum. Line 2 shows a possible path taken by a delocalised SP. This line traverses flat gold and avoids the edges of the nanocavities, thereby avoiding confinement.[18] These delocalised SPs contribute little to SERS enhancement.[12] It is clear from Fig 1(a) that there are many paths that avoid the nanocavity edges, resulting in the presence of many delocalised SPs. The weaker SER spectrum obtained from the external modified arrays (see Fig 1(c)) is consistent with this. The spectrum from the internally modified

Inspection of the Raman spectra in Figs 1(b) and 1(c) shows the presence of a broad, weak background on which the Raman peaks are located. This appears at a frequency at which the metal complex is luminescent. Fig 1(d) outlines the emission spectrum for $[Ru(bpy)_2(Qbpy)]^{2+}$. The spectrum shows that the dye emits from a triplet metal to ligand charge transfer state at 650 nm and is luminescent at 633 nm. This indicates that the observed background originates from laser induced fluorescence. However, Mahajan et al reported that a molecule/electronic continuum coupling model can explain the origin of the background observed in SERS.[2] The model proposes a dipole-dipole coupling between real and image molecules that provides an additional Raman scattering with electron-hole pairs in the metal to generate the background.

Studies of the SERs intensity against angle of incidence were undertaken. Monitoring the change in the intensity of the Raman transition shows that the intensity of the SER band depends upon angle. The intensity profile shows regions of relatively high Raman signal and regions of relatively low Raman signal which vary with $\theta$. Fig 2(a) shows a contour plot of intensity for different energies at varying angles of incidence for the interior modified array. Fig 2(b) shows a

slice of the contour plot as a 2D graph of SER intensity against incident angle for the Raman band at 1.759 eV. The plot shows an initial fall off of intensity, then a peak at approx 20 degrees.

The array has cavities with dimensions $\bar{t}$ = 0.12 that are expected to result in the formation of cavity localised plasmons, localised (rim) plasmons on the edge of the cavity and Bragg plasmons on the surface of the nanocavity array.[6] For the internally modified array the Raman active dye is only present on the internal cavity walls, the top surface is blocked with 1-nonanethiol which, by comparison with the ruthenium complex, contributes very little to the Raman signal.[17] The studied Raman mode at 1.759 eV is attributed to the complex, not the alkane thiol. This enables study of the angle dependence of the SERS spectrum where the enhancement is due only to the plasmons located in the cavity. Each plasmon mode has a unique field distribution within the substrate. The intensities of the plasmons vary as a function of both θ and the frequency of incident EM radiation.[6] Both experimental and theoretical studies have indicated that the absorption energy of such cavity related plasmons change as a function of θ for angle of incidence.[6,8] Simulated plasmonic intensities for 600 nm gold nanocavities as a function of angle (with respect to incident excitation) and cavity size have been reported.[6] The dependence of the plasmon energies demonstrated that the energy of these plasmon modes was sensitive to cavity size and cavity height.

Fig 3 shows SER spectra recorded from $[Ru(bpy)_2(Qbpy)]^{2+}$ prepared on the surface of the array only (in contrast to the studies where the probe molecule was present only in the voids of the substrate shown in Fig 2). Fig 3(a) shows a contour plot of intensity for different energies at varying angles of incidence for the exterior modified array. Fig 3(b) shows a slice of the contour plot as a 2D graph of SER intensity against incident angle for the Raman band at 1.759 eV. The plot shows the SER intensity falls steadily as θ moves out from 0. Comparing SER intensity from $[Ru(bpy)_2(Qbpy)]^{2+}$ prepared only in the voids of the nanocavity array to those prepared only on the surface of the substrate shows clear difference. The plasmon energies of the localised and delocalised plasmons may not be the same. This could result in the absence of SERs effect from delocalised plasmons (indicated by line 2 in Fig 1(a)). It can be inferred from our measurements that a steadily decreasing profile is indicative of localised surface plasmon assisted Raman scattering. Examining the spectral profile of the SER from the surface bound $[Ru(bpy)_2(Qbpy)]^{2+}$ molecule and comparing it to SER from void bound $[Ru(bpy)_2(Qbpy)]^{2+}$ molecules shows important differences. Surface bound SER shows a Raman profile that consists of a larger background compared to a void based SER Raman spectrum. This difference in background is indicative of a different SER mechanism. The surface bound luminescence been less effectively quenched compared to the SER from the void based molecules. This is consistent with the greatest luminescence intensity observed for monolayers of the dye at the top surface as described by Jose et al.[17]

In conclusion, the angle dependence of SERS was investigated for two types of modified nanocavity arrays. The internally modified array had a Raman active dye placed only on the internal walls of the cavities. The externally modified array had dye placed only on the flat surface of the array, leaving the cavity walls blank. The Raman signals obtained from each array differed in intensity and this implies that different types of plasmons enhance the Raman signal. In the case of the internally modified array the SERS is attributed to void (Bragg) plasmons and in the case of the externally modified array the SERS is attributed to surface plasmons. The

difference in the angle dependence plots for each array also implies that different types of plasmons are responsible for the SERS spectra obtained from the arrays.

**References**


[1]B. Jose, R. Steffen, U. Neugebauer, E. Sheridan, R. Marthi, R.J. Forster, and T.E. Keyes, Phys. Chem. Chem. Phys. **11**, 10923 (2009).

[2]S. Mahajan, R.M. Cole, J.D. Speed, S.H. Pelfrey, A.E. Russell, P.N. Bartlett, and J.J. Baumberg, J. Phys. Chem. C **114**, 7242 (2010).

[3]A. M. Schwartzberg, C. D. Grant, A. Colcott, C. E. Talley, T. R. Huser. R. Bogomolni, and J. Z. Zhang, J. Phys. Chem. B **108**, 19191 (2004).

[4]S. Mahajan, M. Abdelsalam, Y. Suguwara, S. Cintra, A. Russell, J. Baumberg, and P. Bartlett, Phys. Chem. Chem. Phys. **9**, 104 (2007).

[5]E. Cortes, N. G. Tognalli, A. Fainstein A, M. E. Vela, and R. C. Salvarezza, Phys. Chem. Chem. Phys. **11**, 7469 (2009).

[6] T. A. Kelf, Y. Sugawara, R. M. Cole, J. J. Baumberg, M. E. Abdelsalam, S. Cintra, S. Mahajan, A. E. Russell, and P. N. Bartlett, Phys. Rev. B **74**, 245415 (2006).

[7]C.Y. Chan, J.B. Xu, M.Y. Waye, and H.C. Ong, Appl. Phys. Lett. **96**, 033104 (2010).

[8]Y. Sugawara, T. A. Kelf, J. J. Baumberg, M. E. Abdelsalam, and P. N. Bartlett, Phys. Rev. Lett. **97,** 266808 (2006).

[9]J. J. Baumberg, T. A. Kelf, Y. Sugawara, S. Cintra, M. E. Abdelsalam, P. N. Bartlett, and A. E. Russell, Nano Lett. **5**, 2262 (2005).

[10]F. Lordan, J. H. Rice, B. Jose, R. J. Forster, and T. E. Keyes, Appl. Phys. Lett. **97**, 153110 (2010).

[11]M. E. Abdelsalam, S. Mahajan, P. N. Bartlett, J J. Baumberg, and A E. Russell, J. Am. Chem. Soc., 129, 7399 (2007)

[12]S. Mahajan, R. M. Cole, B. F. Soares, S. H. Pelfrey, A. E. Russell, J. J. Baumberg, and P. N. Bartlett, J. Phys. Chem. C **113**, 9284 (2009)

[13]S. Mahajan, J. J. Baumberg, A.E. Russell, and P. N. Bartlett, Phys. Chem. Chem. Phys. **9** 6016 (2007)

[14]P. D. Lacharmoise, N. G. Tognalli, A. R. Goñi, M. I. Alonso, A. Fainstein, R. M. Cole, J. J. Baumberg, J. Garcia de Abajo, and P. N. Bartlett, Phys. Rev. B **78**, 125410 (2008)

[15]R. M. Cole, S. Mahajan, P. N. Bartlett, and J. J. Baumberg, Optics Express, 17, 13298 (2009).

[16]R. J. Forster, Y. Pellegrin, D. Leane, J. L. Brennan, and T. E. Keyes, J. Phys. Chem. C, **111**, 2063 (2007)

[17]B. Jose, C. T. Mallon, R. J. Forster, and T. E. Keyes, Phys. Chem. Chem. Phys., In print, (2011).

[18]L. S. Live, M. P. Murray-Methot, and J. F. Masson, J. Phys. Chem. C, **113**, 40 (2009)

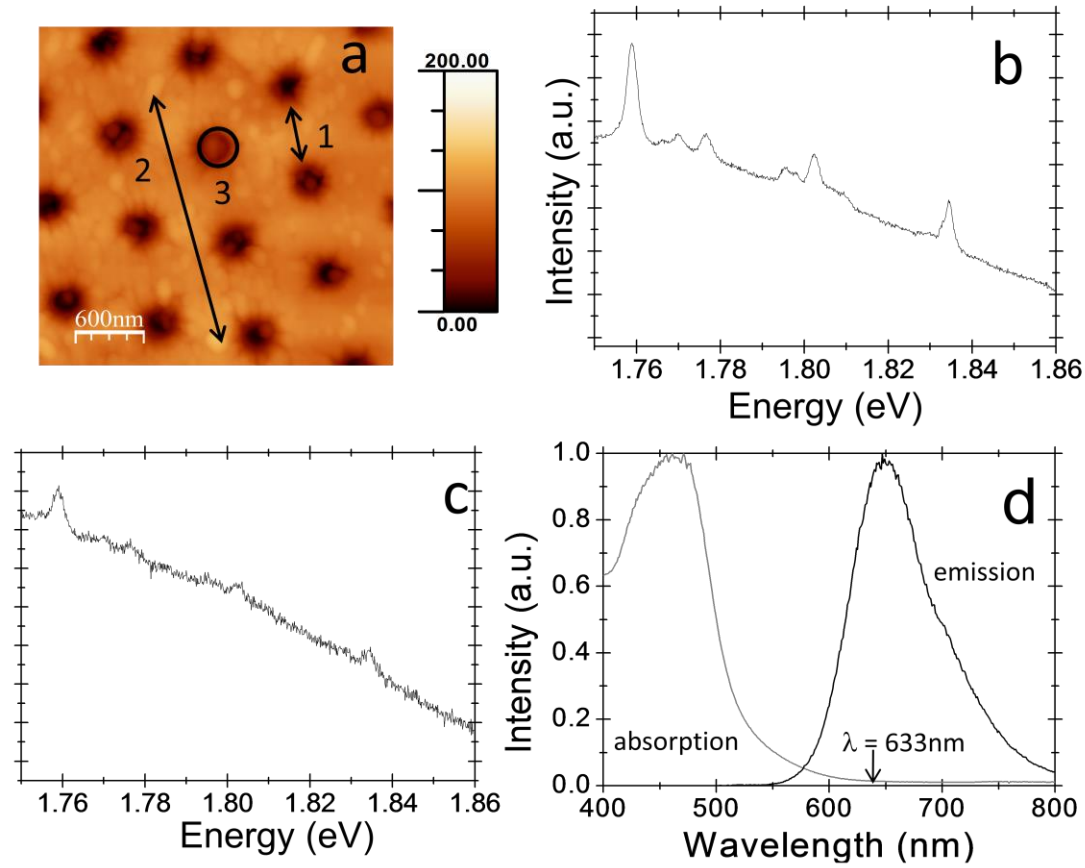


Fig 1. (a) AFM image of the array showing the presence of a regular array of cavities across the sample. The red lines schematically represent examples of 1) localised surface plasmons, 2) delocalised surface plasmons and 3) void plasmons, (b) SERs spectrum taken from dye placed in the voids of the sample, (c) SERs spectrum recorded from dye placed on the surface of the nanovoid cavity array. Excitation wavelength 633 nm, laser power 10 mW, (d) UV-visible absorption and emission spectrum of $[Ru(bpy)2(Qbpy)]^{2+}$ in 1mM methanol.

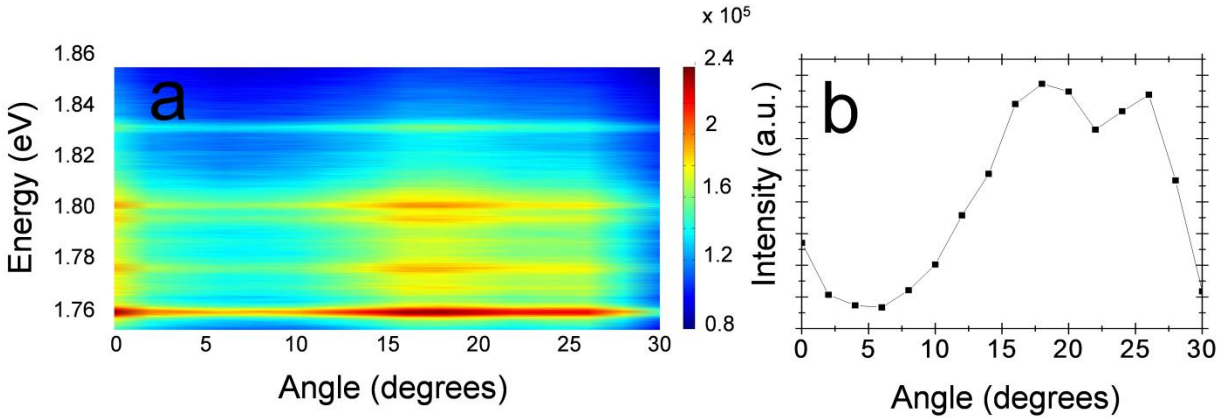


Fig 2. (a) Raman contour plot showing intensity for different energies at varying angles of incidence for the interior modified array, (b) a plot of Raman intensity as a function of angle for the Raman band at 1.759eV.

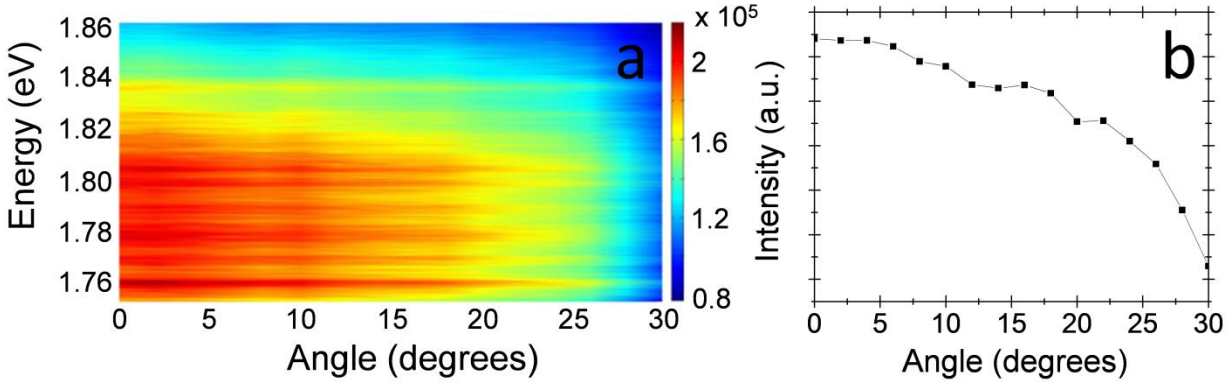


Fig 3. (a) Raman contour plot showing intensity for different energies at varying angles of incidence for the exterior modified array, (b) a plot of Raman intensity as a function of angle for the Raman band at 1.759eV.